Supporting Information

Ito et al. 10.1073/pnas.1118876109

SI Materials and Methods

Plant Materials and Growth Conditions. The Colombia-0 (Col-0) accession was used as a wild type for all experiments. The *ft-101* mutant (a kind gift from K. Goto, Research Institute for Biological Sciences, Okayama, Japan) was described previously (1). To generate *FBH1*, *FBH2*, *FBH3*, and *FBH4* overexpressing transgenic plants, the coding regions of each *FLOWERING BHLH* (*FBH*) gene were amplified from cDNA derived from long-day (LD)-grown wild-type plants using the following primers: 5′-CACCATGCAATCCACTCATATAAGCGG-3′ and 5′-TTGTTCTTCTTTAGGTTTGCATTTGCATCTC-3′ for *FBH1*; 5′-CACCATGCAACCAACATCCGTCGGTAGTAGC-3′ and 5′-TCATTATTGTTCTTCCTTAGGTATGCATG-3′ for *FBH2*; 5′-CACCATGGAATCAGAATTCCAGCAAC-3′ and 5′-TCACGCACTAGAGCATCTACATC-3′ for *FBH3*; and 5′-CACCATGGATTCAAATAATCATCTCTAC-3′ and 5′-CTATATTGACTTCTTCTCCTTG-3′ for *FBH4*. The amplified *FBH* cDNAs were cloned into the pENTR/D-TOPO vector (Invitrogen). After the sequences of *FBH* genes were confirmed, each *FBH* gene was transferred to the pB7WG2 binary vector (2), which contains the CaMV 35S promoter-driven expression cassette, using Gateway LR clonase II (Invitrogen). These constructs were transformed into wild-type plants (Col-0) possessing either *CONSTANS* (*CO*)*:GUS* or *FLOWERING LOCUS T* (*FT*)*:GUS* reporter genes (a kind gift from K. Goto) (1) by conventional *Agrobacterium* (strain: ABI) floral-infiltration methods (3). Transformants were selected on culture media containing Basta (Sigma), and all experiments were carried out using T_3–T_4 homozygous plants that have a single T-DNA insertion. To obtain *35S:FBH1* in an *ft-101* line, *35S:FBH1* #24 plant was crossed to the *ft-101* mutant. Several independent lines that are homozygous for both the *35S:FBH1* transgene and the *ft-101* mutation were obtained from F_3 and F_4 generations and showed similar phenotypes. To generate a FLAG epitope-tagged FBH1 fusion construct (designated as *35S:FLAG-FBH1*), the oligonucleotides encoding 3× FLAG sequences (5′-GATAGCCATGGATTACAAGGATCATGATGGTGATTACAAGGATCACGACATCGACTACAAGGATGACGATGACAAGGGTGGAGCTCGGTACC-3′; restriction enzyme sites are denoted by underlining) were synthesized, further amplified by PCR using the primers (5′-GATAGCCATGGATTACAAGGATC-3′ and 5′-GGTACCGAGCTCCACCCTTG-3′), and cloned into the unique NcoI-KpnI sites of the pRTL2 vector (4). The coding region of *FBH1* was amplified using the primers 5′-CTCGGTACCCGATGCAATCCACTCATATAAGCGGCG-3′ and 5′-GATGCTAGCTTATTGTTCTTCTTTAGGTTTGCATTTGC-3′, digested by KpnI and NheI and cloned into the KpnI-XbaI sites of pRTL2 (named *pRTL2-FLAG-FBH1*). To generate the *FBH1* promoter driven *3×FLAG-FBH1* construct, the CaMV 35S promoter (located between the EcoRV and NcoI sites) in *pRTL2-FLAG-FBH1* was replaced by 1.35 kb of the *FBH1* promoter and the 5′-UTR fragment (which was amplified using 5′-TTGTCGACCTTGATATCGTGTTCCTTTTTACCTCA-3′ and 5′-TTGGATCCCATGGGGGTCTCCACCGGAGAATGT-3′ primers). Expression cassettes from both pRTL2-derived plasmids were cloned into the pPZP221 binary vector (5). Then T-DNAs possessing both *35S* and *FBH1* promoter-driven *3×FLAG-FBH1* expression constructs were integrated into the wild-type genome. *fbh2-1* [SALK_063655; T-DNA insertion was located at the position of +104 (the translation initiation site was counted as +1) (Fig. S3*J*)] and *fbh3-1* [SAIL_551_B11; T-DNA insertion was located at the position of +670 to +687 (Fig. S6*A*)] alleles were obtained from the Arabidopsis Biological Resource Center. For making the artificial microRNA (amiRNA) constructs that specifically reduce the amount of either *FBH1* or *FBH4* mRNA, candidate sequences and primers were designed using the WMD3 Web site (http://wmd3.weigelworld.org/cgi-bin/webapp.cgi?page=Home;project=stdwmd) (6). The amiRNA vector pRS300 was obtained from Addgene (http://www.addgene.org/). Using the instructions on the Web site, we introduced specific *FBH1*- or *FBH4*-targeted microRNA sequences into the original miR319 backbone plasmid (pRS300) by PCR-mediated mutagenesis (Table S1). The resulting amiRNA specific to *FBH1* (designated as *amiR-FBH1-1* and *amiR-FBH1-2*) was then cloned into the EcoRI-BamHI sites of the pRTL2 vector, and the expression cassettes (*35S:amiR-FBH1-1* or *35S:amiR-FBH1-2*) were transferred into the HindIII site of the pPZP221 binary vector. The amiRNA specific to *FBH4* (named *amiR-FBH4-1* and *amiR-FBH4-3*) was cloned into the pENTR/D-TOPO vector, and after the LR reaction each *amiR-FBH4* fragment was transferred to the pH7WG2 binary vector (2). To obtain multiple mutant lines, either the *35S:amiR-FBH1-1* or the *35S:amiR-FBH1-2* construct was transformed into the *fbh2-1* mutant line, and then subsequently the *35S:amiR-FBH1-2*, *fbh2-1* double-mutant line was crossed with the *fbh3-1* mutant line to make a triple mutant. Finally, either the *35S:amiR-FBH4-1* or the *35S:amiR-FBH4-3* construct was transformed to the *35S:amiR-FBH1-2*, *fbh2-1*, *fbh3-1* triple-mutant line. All homozygote lines were selected by several antibiotic-resistant markers and confirmed by genomic PCR.

The coding regions of the *PtFBH1* gene (estExt_fgenesh4_pg.C_410126) were amplified from cDNA derived from young poplar (*Populus trichocarpa*; genotype: Nisqually 1) leaves grown in a greenhouse at the University of Washington using the primers 5′-CACCATGCATCCAGCACCGGCAGGAAGCA-3′ and 5′-TTATTCTTTAGCCATGCATTTGCAT-3′. The amplified cDNA was cloned into the pENTR/D-TOPO vector (Invitrogen). The rice (*Oryza sativa*; cultivar: Nipponbare) EST clone (OSJNEf08L), which contains the full length of *OsFBH1* (Os08g39630), was obtained from the Arizona Genomic Institute (University of Arizona). After the *OsFBH1* cDNA fragment was excised by NotI and XhoI, the fragment was cloned into the pENTR-Keiko vector (pENTR-D/TOPO vector containing the pBluescriptII multicloning sites, a kind gift from K. Torii, University of Washington, Seattle, WA). After the sequences of *PtFBH1* and *OsFBH1* genes were confirmed, these cDNA were transferred to the pB7WG2 binary vector (2) using Gateway LR clonase II (Invitrogen). These binary constructs were transformed into wild-type plants (Col-0) possessing the *CO:GUS* reporter gene by conventional *Agrobacterium* (strain: ABI) floral-infiltration methods (3).

Yeast One-Hybrid Analysis. All reporter strains were generated in the yeast strain YM4271 according to the manufacturer's protocol (Clontech). A series of truncated *CO* promoter fragments were amplified by PCR from Col-0 genomic DNA using the following primers: 5′-CACGATATCTCTAACCTTTGTATAGGTAGTCAACCC-3′ and 5′-GGGAATTCAAAGCTTATATCTGGTGTGAGAGAATAAGTAGAGG-3′ for the −509 to −1 region; 5′-TGCCTGCAACACCATGGCATTATCC-3′ and 5′-GGGAATTCAAAGCTTATATCTGGTGTGAGAGAATAAGTAGAGG-3′ for the −288 to −1 region; and 5′-CAACGAAGAAGTGCATAGGAGG-3′ and 5′-GGGAATTCAAAGCTTATATCTGGTGTGAGAGAATAAGTAGAGG-3′ for the −196 to −1 region). The amplified DNA fragments were cloned into the pENTR5′-TOPO vector (Invitrogen) and then transferred to pMW3 [pLacZi vector containing the gateway cassette (7)] following the manufacturer's protocol (Invitrogen). The transformation of the circadian-clock–

regulated transcription factor library was performed in a 96-well format as previously described (8). To generate translational fusions to the GAL4 activation domain (AD), the coding sequences of FBH genes were cloned in pENTR/D-TOPO and subsequently transferred into pDEST22 (Invitrogen). For the control plasmid, pEXP-AD502 (Invitrogen) was used as previously described (8). For expressing the AD-CDF1 fusion protein, the pACT2-CDF1 plasmid was used (9). Note that both pDEST22 and pACT2 are prey vectors, but the expression level of AD fusions in pACT2 is usually higher than that in pDEST22. Transformation of AD constructs into the reporter strains and measurement of the β-galactosidase activity were performed in a 96-well format as previously described (8). Four tandem repeats of E-box elements (designated as 4 × E-box) or four tandem repeats of mutated E-box elements (designated as 4 × Mut. E-box) were generated by the annealing of the following complementary forward and reverse oligonucleotides. The forward oligonucleotides are 5′-CCGGAATTCAGTATGG**CAAGTG**GCAAAACAGTATGG**CAAGTG**GCAAAACAGTATGG**CAAGTG**GCAAAACAGTATGG**CAAGTG**GCAAAACGGTACCCCG-3′ for 4 × E-box (the E-box element is in boldface type) and 5′-CCGGAATTCAGTATGG**GTAGTG**GCAAAACAGTATGG**GTAAGT**GGCAAAACAGTATGGGTAGTGGCAAAACAGTATGG**GTAGTG**GCAAAACGGTACCCCG-3′ for 4 × Mut (the mutated E-box element is in boldface type). Annealed fragments were digested with EcoRI and KpnI and cloned into EcoRI-KpnI sites of pLacZi (Clontech), and the resulting plasmids were confirmed by sequencing.

Electrophoretic Mobility Shift Assay. We used affinity-purified 6 × His-FBH1 and 6 × His-FBH2 recombinant proteins for the electrophoretic mobility shift assay (EMSA). To generate 6 × His-FBH1 and 6 × His-FBH2 proteins, the coding regions of *FBH1* and *FBH2* were amplified by PCR using 5′-CATGAATTCATGCAATCCACTCATATAAGCG-3′ and 5′-TAACTCGAGTTATTGTTCTTCTTTAGGTTTGC-3′ primers for *FBH1* and 5′-CATGAATTCATGCAACCAACATCCGTCGGTAG-3′ and 5′-TAACTCGAGTTATTGTTCTTCCTTAGGTATGC-3′ primers for *FBH2*. Restriction sites are underlined. The amplified fragments were digested with EcoRI and XhoI and then cloned into the EcoRI-XhoI sites of pET28a (Novagen). After the sequences of *FBH1* and *FBH2* were confirmed, the resulting pET28a-FBH1 and pET28a-FBH2 plasmids were transformed into the *Escherichia coli* strain BL21-CodonPlus (DE3) (Stratagene). Both 6 × His-FBH1 and 6 × His-FBH2 proteins synthesized in the *E. coli* were purified using the Ni-column according to the manufacturer's protocol (Novagen). The EMSA procedure was described previously (10).

Flowering-Time Experiment. For flowering-time analysis, seeds were sown on the soil (Sunshine Mix #4; Sun Gro Horticulture) directly and stratified for 2–3 d at 4 °C in darkness to synchronize the timing of germination. Plants were grown at 22 °C under LD (16 h light/8 h dark) or short-day (SD) (8 h light/16 h dark) conditions. Light was provided by full-spectrum white fluorescent light bulbs (F017/950/24′′ Octron; Osram Sylvania) with a fluence rate of 60–90 $\mu mol \cdot m^{-2} \cdot s^{-1}$ in LD and 75–115 $\mu mol \cdot m^{-2} \cdot s^{-1}$ in SD. Flowering time was measured by counting the number of rosette and cauline leaves on the main stem when they bolted. The experiments were repeated at least twice with at least six individual plants, and similar results were obtained. The results are means ± SEs of means (SEM).

RNA Preparation and Gene Expression Analyses (Quantitative PCR and RT-PCR). Seedlings were grown on plates containing 1× Linsmaier and Skoog (LS) media (Caisson) and 3% sucrose under LD, SD, or 12 h light/12 h dark conditions for 10 d and harvested at 3-h intervals from 1 h after the onset of light (ZT 1) to ZT 22 or transferred to continuous light conditions then harvested at 4-h intervals from ZT 0 for 3 d. To quantify the mRNA of the genes involved in flowering regulation, total RNA was isolated from seedlings using an illustra RNAspin Mini kit (GE Healthcare). To synthesize cDNA, 2 μg of total RNA was reverse-transcribed using an iScript cDNA synthesis kit (Bio-Rad). cDNA was diluted to 50–60 μL with water, and 2 μL each of diluted cDNA was used for quantitative PCR (qPCR) and RT-PCR analyses. The qPCR was performed in the buffer consisting of 1× ExTaq buffer (Takara Bio), 0.1 mM Hepes–Na (pH 7.5), 1× SYBR-Green (Molecular Probes), 10 nM fluorescein (Bio-Rad), 0.1% (wt/vol) Tween-20, 5% (vol/vol) DMSO, 100 μg/mL BSA, 0.2 mM dNTPs, 250 nM primers, and 1 U Taq DNA polymerase (New England Biolabs) using a Bio-Rad MyiQ real-time detection system. The primer sequences used for PCR are shown in Table S2. *Isopentenyl pyrophosphate/dimethylallyl pyrophosphate isomerase* (*IPP2*) was used as an internal control for normalization (11). To amplify *CO*, *FBH4*, *FKF1*, *CDF1*, and *CDF2*, we used the following three-step PCR program: 1 min at 95 °C, followed by 40–50 cycles of 10 s at 95 °C, 20 s at 52–55 °C, and 20 s at 72 °C. To amplify the rest of gene, we used the following two-step PCR program: 1 min at 95 °C, followed by 40–50 cycles of 10 s at 95 °C and 20 s at 60 °C. Each data value shown in the figures (Figs. 2, 4, S1–S6, and S9) is the average derived from three biological replicates, and the value of each sample in each replicate is the average of values obtained from two technically replicated PCR reactions. Error bars indicate the SEM from three independent biological replicates. RT-PCR was performed to check whether intact *FBH3* transcripts exist in the *fbh3-1* mutant (Fig. S6*B*), using the following sets of primers: (a—5′-CACCATGGAATCAGAATTCCAGCAAC-3′; b—5′-CGCACTAGAGCATCTACATCTTG-3′; c—5′-TAGCATCTGAATTTCATAACCAATCTCGAT-3′; and d—5′-GACCTCCAGATTGGGTCCTAG-3′).

To detect *PtFBH1* and *OsFBH1* transcripts in *Arabidopsis* plants expressing *35S:PtFBH1* and *35S:OsFBH*, the following sets of primers were used: 5′-GTTTGTATGAAACGGGTAGTGG-3′ and 5′-CTCCATATTTGGCGGCATATACTC-3′ for *PtFBH1* and 5′-ATGTACGGCTCGCCGGTTTCCAAGGATCTG-3′ and 5′-AGAAGACGTTGTCGGCGTCG-3′ for *OsFBH1*.

Analysis of Tissue Expressions (GUS Staining). For the construction of *FBH1*, *FBH3*, and the *FBH4:GUS* reporter gene, the 5′ upstream region of the *FBH1* sequence (−1313 to −1; the translation initiation site was counted as +1), *FBH3* (−1679 to +45), and *FBH4* (−1559 to +87) were amplified from Col-0 genomic DNA using the following primers: 5′-GGAGTCGACCAACACATTTGGGGCTGGAGATGAAG-3′ and 5′-CCGGATCCGGGGTCTCCACCGGAGAATGTC-3′ for *FBH1*; 5′-ATAGTCGACGCCCAAGGCATTAATCGGTATCAAAC-3′ and 5′-CTGGGATCCATGATCGTGGAGAAGGAAGTGATGTTGC-3′ for *FBH3*; and 5′-AGAGTCGACGTCACTGTATAATCCATCGACCACTAAGG-3′ and 5′-CAACAGATCTGGCGAGAACAGAGCTCGGAGCTGATC-3′ for *FBH4* (restriction sites are underlined) and cloned into SalI-BamHI or SalI-BglI sites of the pBI101 binary vector (Clontech). Transgenic lines carrying the *CO:GUS* or the *FT:GUS* transgene (a kind gift from K. Goto) were described previously (1). Transgenic plants were grown under LD conditions for 12 d and fixed with cold 90% acetone on ice for 10–15 min. Subsequently, plants were incubated at 37 °C in the staining buffer [0.5 mM X-Gluc, 50 mM sodium phosphate (pH 7.2), 0.5 mM of $K_4Fe(CN)_6$, and 0.5 mM $K_3Fe(CN)_6$]. After staining, the samples were bleached and dehydrated with a sequence of buffers: 30% ethanol, fixing solution (50% ethanol, 5% acetic acid, and 3.7% formaldehyde), and 80% and 100% ethanol for 30 min each. The staining patterns of GUS activity of more than 20 individual T_1 transgenic plants were analyzed, and the data from the T_2 and T_3 population plants that showed the representative staining patterns of T_1 populations are shown.

β-Estradiol-Mediated Induction Experiment. To generate *pER8-FBH1* and *pER8-FBH2* constructs that contain the estradiol-in-

ducible *FBH1* or *FBH2* expression cassettes, the full length of *FBH1* and *FBH2* cDNAs were amplified using the following primers: 5′-CATCTCGAGATGCAATCCACTCATATAAGC-GGC-3′ and 5′-TAAACTAGTTTATTGTTCTTCTTTAGGTT-TGC-3′ for *FBH1* and 5′-CATCTCGAGATGCAACCAACA-TCCGTCGGTAG-3′ and 5′-TAAACTAGTTTATTGTTCTT-CCTTAGGTATGCATG-3′ for *FBH2* (restriction sites are underlined). Each *FBH1* and *FBH2* fragment was inserted into the XhoI-SpeI sites of the binary vector *pER8* (a kind gift from N.-H. Chua, The Rockefeller University, New York, NY) (12). After we verified the accuracy of the sequences, these constructs were transformed to the wild-type plants by the conventional *Agrobacterium* method. To analyze the effect of β-estradiol application on *pER8-FBH1* and *pER8-FBH2* plants, 10-d-old seedlings grown on a filter paper (Whatman 1001–070) placed on LS media were transferred to the media containing 5 μM of β-estradiol plate at ZT 0. As a mock treatment, seedlings were transferred to the LS media containing the same amount of EtOH (the solvent of β-estradiol) at the same time. All seedlings were harvested at 3-h intervals for 2 d from ZT 1.

Immunoblot Analysis. Total crude protein was extracted from frozen-ground seedlings in the extraction buffer [50 mM sodium phosphate (pH 7.0), 100 mM NaCl, 10% (wt/vol) glycerol, 5 mM EDTA, 0.1% (wt/vol) Triton X-100, 5 mM DTT, 50 μM MG-132, 0.1% SDS, 0.5% sodium deoxycholate and complete protease inhibitor mixture tablets (Roche)]. The supernatant was collected after centrifugation at 21,000 × *g* for 10 min. Then protein samples were separated by 12–15% SDS/PAGE gels and transferred to nitrocellulose membranes (for each sample, 5–10 μg of total protein was used). Membranes were blocked using a blocking buffer [1×TBS milk: 5% skim milk, 9.2 mM Tris·HCl (pH 7.6) and 137 mM NaCl] at 25 °C for 1 h, and the 3×FLAG epitope-tagged FBH1 fusion protein was detected using anti-FLAG antibody (Sigma). Horseradish-peroxidase–conjugated anti-mouse IgG (Thermo Fisher Scientific) was used as a secondary antibody, and Super Signal West Pico and Femto Chemiluminescent substrate kits (Thermo Fisher Scientific) were used to detect signals derived from the antibodies. All experiments were performed at least three times with independent biological replicates. As loading references, the same nitrocellulose membrane was stained by Ponceau S, and RuBisCo large subunit bands are shown in Fig. S3 as loading controls.

Chromatin Immunoprecipitation Assays. Procedures of cross-linking and isolation of chromatin were performed essentially as described previously (13). Briefly, 3 g (fresh weight) of 2-wk-old seedlings were harvested at a specific ZT time and treated with 1% formaldehyde under vacuum for 15 min at room temperature. The cross-linking reaction was stopped by adding glycine to a final concentration of 0.125 M under vacuum for 5 min. The seedlings were rinsed with water, frozen in liquid nitrogen, and ground to a fine powder. Then nuclei were extracted, lysed in the nuclei lysis buffer [50 mM Tris·HCl (pH 8.0), 10 mM EDTA, 1% SDS, 1 mM PMSF, 5 mM benzamidine, 50 μM MG-132, and complete protease inhibitor mixture tablets), and sonicated to shear DNA to an average size of 500–1,000 bp. The chromatin solution was diluted 10-fold with chromatin immunoprecipitation (ChIP) dilution buffer [16.7 mM Tris·HCl (pH 8.0), 167 mM NaCl, 1.1% (wt/vol) Triton X-100, 1.2 mM EDTA, 1 mM PMSF, 5 mM benzamidine, 50 μM MG-132, and complete protease inhibitor mixture tablets]. Immunoprecipitation was performed using Dynabeads Protein G (Invitrogen). The beads were pretreated with either anti-FLAG antibody (Sigma) or mouse IgG whole molecule (Jackson ImmunoResearch) and incubated with chromatin solution in an ultrasonic water bath for 20 min at 4 °C. Incubation of the beads with mouse IgG pretreatment served as the mock control. After washing with low-salt buffer [20 mM Tris·HCl (pH 8.0), 150 mM NaCl, 0.2% SDS, 0.5% (wt/vol) Triton X-100, 2 mM EDTA], high-salt buffer [20 mM Tris·HCl (pH 8.0), 500 mM NaCl, 0.2% SDS, 0.5% (wt/vol) Triton X-100, 2 mM EDTA], and TE buffer [10 mM Tris·HCl (pH 8.0), 1 mM EDTA], immunocomplexes were eluted from beads and reverse cross-linked by boiling for 10 min with 10% Chelex resin (Bio-Rad). One tenth of chromatin solution of each sample was used for the total input fraction, which was also treated in the same procedure. Eluted samples are incubated with a Proteinase-K at 50 °C to digest all proteins. DNA was diluted to 200 μL with TE buffer, and 2-μL aliquots were used for qPCR. The forward and reverse primer pairs that were used to amplify the genome sequence designated as *CO* amplicon 1 to amplicon 9 are shown in Table S3. A two-step qPCR program [see *RNA Preparation and Gene Expression Analyses (Quantitative PCR and RT-PCR)*] was used to amplify all amplicons. The immunoprecipitation efficiency (%) against the total input was calculated for each amplicon using the following formula: $0.1 \times 2^{(\text{Ct input-Ct ChIP})} \times 100$.

Phylogenetic Analysis. At first, the following FBH protein sequences were retrieved from The *Arabidopsis* Information Resource (http://www.arabidopsis.org), the Rice Genome Annotation Project (http://rice.plantbiology.msu.edu), and Phytozome (http://www.phytozome.net) for the following six overexpressed basic helix–loop–helix (bHLH) transcription factors: At1g35460 (FBH1), At4g09180 (FBH2), At1g51140 (FBH3), At2g42280 (FBH4), estExt_fgenesh4_pg.C_410126 (=POPTR_0013s11200), and Os08g39630. HMMalign was used to align the sequences to the PFAM hidden Markov model profile (pHMM) for the bHLH family (http://pfam.sanger.ac.uk). A pHMM of the alignment was made using HMMbuild (14), and HMMsearch (14) was used to query this pHMM against the Plant Transcription Factor Database (15) for bHLH sequences from *Arabidopsis thaliana*, *Populus trichocarpa*, *Vitis vinifera*, *Solanum lycopersicum*, *Oryza sativa*, and *Zea mays*. Preliminary phylogenetic analyses placed 42 sequences in the in-group, and another 18 out-group sequences from only *A. thaliana* and *O. sativa* were included to show congruence with the Pires and Dolan tree (16), and all other sequences were discarded to increase readability in the published phylogenetic tree. A total of 226 unambiguous aligned amino acid positions covering the bHLH region and three additional areas conserved among in-group sequences were used for phylogenetic analysis.

The Jones, Taylor, and Thornton (17) model (JTT) was determined as the best-fit amino acid substitution model using the Akaike information criterion as implemented in ProtTest (18). Maximum-likelihood (ML) analysis was performed in the program GARLI-2.0 (19) using the JTT model with default parameters (empirical state frequencies, four rate categories, and estimates of both the model of rate heterogeneity and invariant sites). To verify convergence, five runs of two replicates were run before the same likelihood score was recovered for five times for the best tree. One hundred bootstrap (20) replicates were performed using the parameters above. The program SumTrees (21) was used to calculate bootstrap percentages and place them on the best ML tree. Trees were visualized using the program FigTree (http://tree.bio.ed.ac.uk/software/figtree).

1. Takada S, Goto K (2003) Terminal flower2, an Arabidopsis homolog of heterochromatin protein1, counteracts the activation of *flowering locus T* by constans in the vascular tissues of leaves to regulate flowering time. *Plant Cell* 15: 2856–2865.
2. Karimi M, Inzé D, Depicker A (2002) GATEWAY vectors for Agrobacterium-mediated plant transformation. *Trends Plant Sci* 7:193–195.
3. Zhang X, Henriques R, Lin SS, Niu QW, Chua NH (2006) Agrobacterium-mediated transformation of Arabidopsis thaliana using the floral dip method. *Nat Protoc* 1:641–646.

4. Carrington JC, Freed DD, Leinicke AJ (1991) Bipartite signal sequence mediates nuclear translocation of the plant potyviral NIa protein. *Plant Cell* 3:953–962.
5. Hajdukiewicz P, Svab Z, Maliga P (1994) The small, versatile pPZP family of Agrobacterium binary vectors for plant transformation. *Plant Mol Biol* 25:989–994.
6. Schwab R, Ossowski S, Riester M, Warthmann N, Weigel D (2006) Highly specific gene silencing by artificial microRNAs in Arabidopsis. *Plant Cell* 18:1121–1133.
7. Deplancke B, et al. (2006) A gene-centered C. elegans protein-DNA interaction network. *Cell* 125:1193–1205.
8. Pruneda-Paz JL, Breton G, Para A, Kay SA (2009) A functional genomics approach reveals CHE as a component of the *Arabidopsis* circadian clock. *Science* 323: 1481–1485.
9. Imaizumi T, Schultz TF, Harmon FG, Ho LA, Kay SA (2005) FKF1 F-box protein mediates cyclic degradation of a repressor of *CONSTANS* in *Arabidopsis*. *Science* 309:293–297.
10. Song YH, et al. (2008) Isolation of CONSTANS as a TGA4/OBF4 interacting protein. *Mol Cells* 25:559–565.
11. Hazen SP, et al. (2005) *LUX ARRHYTHMO* encodes a Myb domain protein essential for circadian rhythms. *Proc Natl Acad Sci USA* 102:10387–10392.
12. Zuo J, Niu QW, Chua NH (2000) Technical advance: An estrogen receptor-based transactivator XVE mediates highly inducible gene expression in transgenic plants. *Plant J* 24:265–273.
13. Nelson JD, Denisenko O, Sova P, Bomsztyk K (2006) Fast chromatin immunoprecipitation assay. *Nucleic Acids Res* 34:e2.
14. Eddy SR (1998) Profile hidden Markov models. *Bioinformatics* 14:755–763.
15. Zhang H, et al. (2011) PlantTFDB 2.0: Update and improvement of the comprehensive plant transcription factor database. *Nucleic Acids Res* 39(Database issue):D1114–D1117.
16. Pires N, Dolan L (2010) Origin and diversification of basic-helix-loop-helix proteins in plants. *Mol Biol Evol* 27:862–874.
17. Jones DT, Taylor WR, Thornton JM (1992) The rapid generation of mutation data matrices from protein sequences. *Comput Appl Biosci* 8:275–282.
18. Abascal F, Zardoya R, Posada D (2005) ProtTest: Selection of best-fit models of protein evolution. *Bioinformatics* 21:2104–2105.
19. Zwickl DJ (2006) Genetic algorithm approaches for the phylogenetic analysis of large biological sequence datasets under the maximum likelihood criterion. PhD dissertation (University of Texas, Austin, TX).
20. Felsenstein J (1985) Confidence-limits on phylogenies: An approach using the bootstrap. *Evolution* 39:783–791.
21. Sukumaran J, Holder MT (2010) DendroPy: A Python library for phylogenetic computing. *Bioinformatics* 26:1569–1571.
22. Carretero-Paulet L, et al. (2010) Genome-wide classification and evolutionary analysis of the bHLH family of transcription factors in Arabidopsis, poplar, rice, moss, and algae. *Plant Physiol* 153:1398–1412.

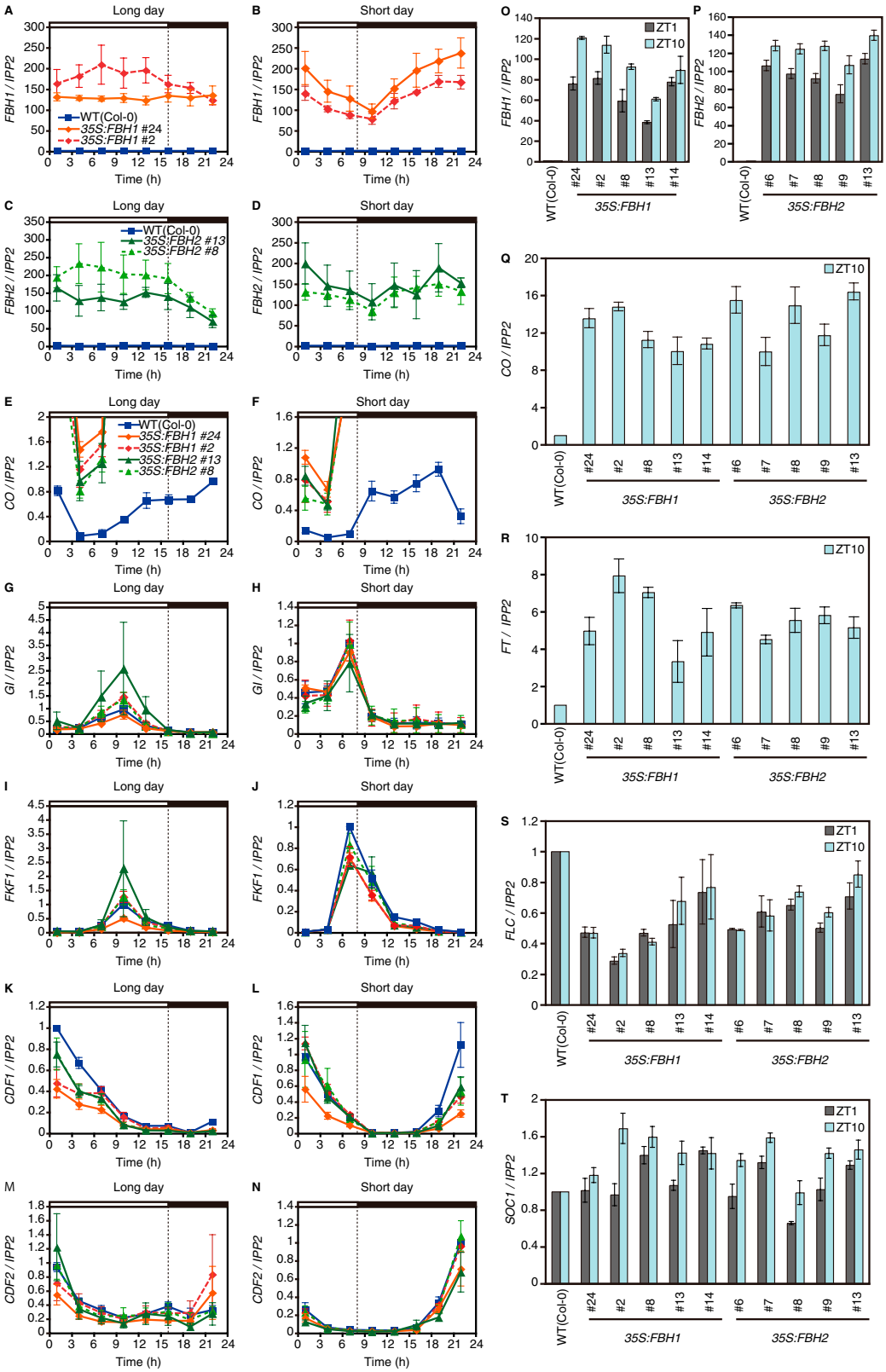

Fig. S1. Expression of photoperiodic flowering pathway genes in several independent *FBH1* and *FBH2* overexpressors. Daily expression patterns of *FBH1* (*A* and *B*), *FBH2* (*C* and *D*), *CO* (*E* and *F*), *GI* (*G* and *H*), *FKF1* (*I* and *J*), *CDF1* (*K* and *L*), and *CDF2* (*M* and *N*) were measured in *35S:FBH1* (#2 and #24), *35S:FBH2* (#8 and #13), and wild-type plants in LD and SD conditions. The scale of the *y* axis of Fig. 2 *D* and *E* was changed to visualize the *CO* mRNA expression levels in wild type under LD (*E*) and SD (*F*) conditions. *FBH1* and *FBH2* levels were normalized to the average value in the wild type (the average value from all of the wild-type time points was set to 1). Other gene expression levels were normalized to the maximum value in wild type (the maximum value of the wild type was set to 1). Bars above the graphs represent light conditions during harvesting samples: white bars represent light periods and black bars represent dark periods.

Legend continued on following page

Expression levels of *FBH1* (*O*), *FBH2* (*P*), *CO* (*Q*), *FT* (*R*), *FLC* (*S*), and *SOC1* (*T*) were analyzed using several independent *35S:FBH1* lines (#24, #2, #8, #13 and #14) and *35S:FBH2* lines (#6, #7, #8, #9 and #13) at 1 h after the onset of light (ZT 1) and at 10 h after the onset of light (ZT 10) under LD conditions. Gray and light blue bar graphs depict the results obtained from ZT 1 and ZT 10 time points, respectively. All of the results were normalized to the values in the wild type (the value of wild type was set to 1). Values represent means ± SEM from three biological replicates.

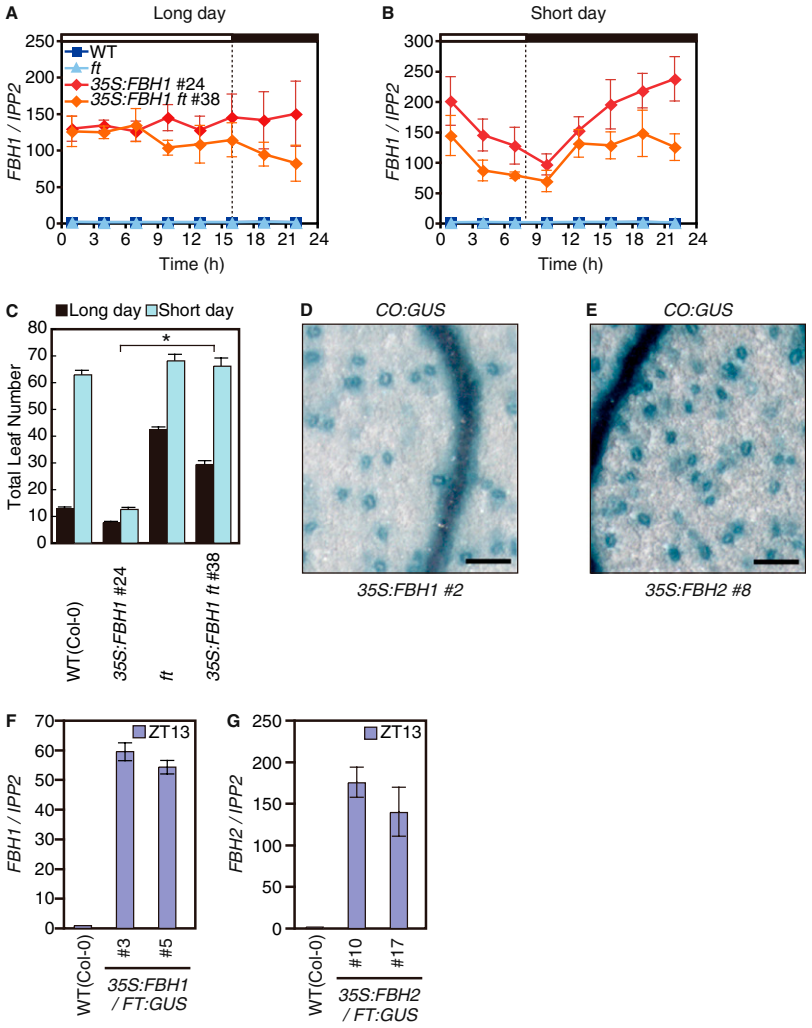

Fig. S2. The flowering phenotype of *35S:FBH1* in the *ft* mutant background and spatial expression patterns of *CO and FT* in the *35S:FBH* plants. (*A* and *B*) Daily expression patterns of *FBH1* in *35S:FBH1* (#24), *35S:FBH1 ft* (#38), *ft*, and wild-type plants were measured in LD and SD. *FBH1* mRNA levels were normalized to the average value in the wild type (the average value from all of the wild-type time points was set to 1). Bars above the graphs represent light conditions during harvesting samples: white bars represent light periods and black bars represent dark periods. Values represent means ± SEM from three biological replicates. (*C*) Flowering phenotype of the *35S:FBH1 ft* plants under different photoperiods. *35S:FBH1* (#24), *35S:FBH1 ft* (#38), wild type, and *ft* mutant plants were grown under both LD and SD conditions, and the total leaf number was counted when they bolted. Error bars denote the ± SEM of at least eight plants per line. Asterisk (*) denotes significant difference ($P < 0.001$) between *35S:FBH1 ft* plants and *ft* plants. The experiments were repeated at least twice using independently established *35S:FBH1 ft* lines, and similar results were obtained. (*D* and *E*) Spatial expression of *CO* in 12-d-old *35S:FBH1* (*D*) and *35S:FBH2* (*E*) seedlings grown under LD conditions. Plants express the *CO:GUS* reporter in the stomata of cotyledons. (Scale bars, 0.1 mm.) (*F* and *G*) Expression levels of *FBH1* and *FBH2* transcripts were measured in two independent *35S:FBH1* lines (#3 and #5) and *35S:FBH2* lines (#10 and #17) in LD. These four lines possess the *FT:GUS* reporter, and they were used to analyze the spatial expression of pattern of *FT* gene in Fig. 2 *Q* and *R*. Ten-day-old seedlings were harvested at 13 h after the onset of light (ZT 13). All of the results were normalized to the values in the wild type (the value of wild type was set to 1). Values represent means ± SEM from three biological replicates.

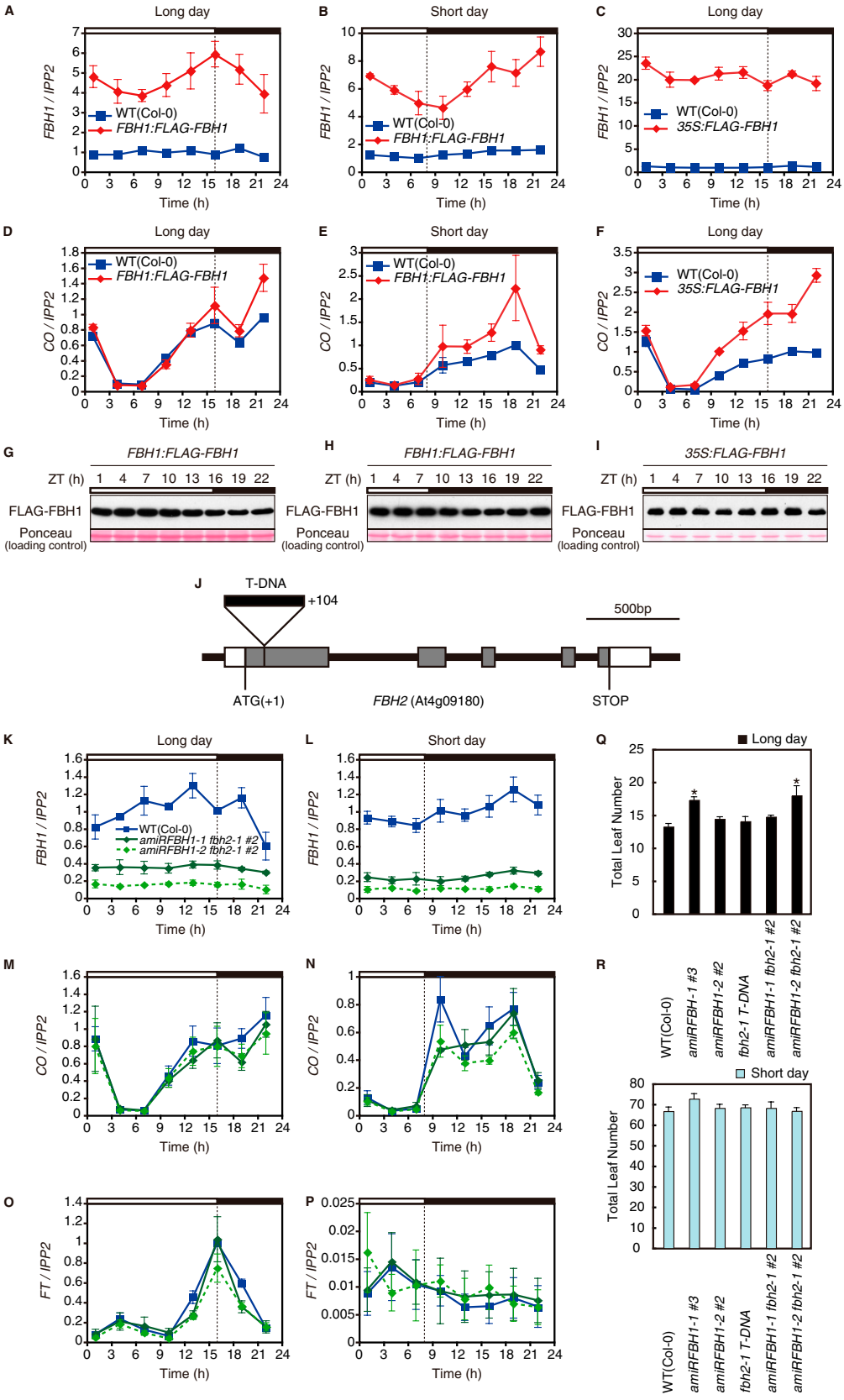

Fig. S3. *FBH1* mRNA and protein expression pattern in *FLAG-FBH1* transgenic plants and the phenotype of *fbh1 fbh2* double-mutant plants. Daily mRNA expression levels of *FBH1* (*A*–*C*) and *CO* (*D*–*F*) were measured in the *FBH1:FLAG-FBH1* line (the line used in Fig. 3 *E* and *F*), the *35S:FLAG-FBH1* line (the line used in Fig. 3 *G* and *H*), and wild-type plants in LD. Daily accumulation patterns of FLAG-FBH1 protein were analyzed in *FBH1:FLAG-FBH1* plants in LD (*G*) and SD (*H*) and in *35S:FLAG-FBH1* plants in LD (*I*) by Western blot. Resolved proteins transferred to the membranes were stained by Ponceau S, and RuBisCo large subunit

Legend continued on following page

bands are shown as a loading control. (*J*) Schematic representation of the *FBH2* locus in the *fbh2-1* mutant. A T-DNA is inserted at the first exon, which is 104 bp downstream of the *FBH1* translation start site. (*K–P*) Daily expression patterns of *FBH1* (*K* and *L*), *CO* (*M* and *N*), and *FT* (*O* and *P*) were measured in two independent *fbh1 fbh2* mutant lines (*amiRFBH1-1 fbh2-1* #2 and *amiRFBH1-2 fbh2-1* #2) and wild-type plants in LD and SD. *FBH1* levels were normalized to the average value in the wild type (the average value from all of the wild-type time points was set to 1). The *CO* and *FT* levels were normalized to the maximum value in wild type (the maximum value of wild type was set to 1). Bars above the graphs and the bands represent light conditions during harvesting samples: white bars represent light periods and black bars represent dark periods. Values represent means ± SEM from three biological replicates. (*Q* and *R*) Flowering phenotypes of each *fbh* single-mutant, *fbh1 fbh2* double-mutant, and wild-type plant were analyzed under different photoperiod conditions. These seedlings were grown in LD and SD, and the total leaf number was counted when they bolted. Error bars denote the SEM of at least eight plants per line. Asterisks (*) denote significant difference ($P < 0.001$) between the indicated *fbh* mutant plants and wild-type plants. The experiments were repeated at least twice, and similar results were obtained.

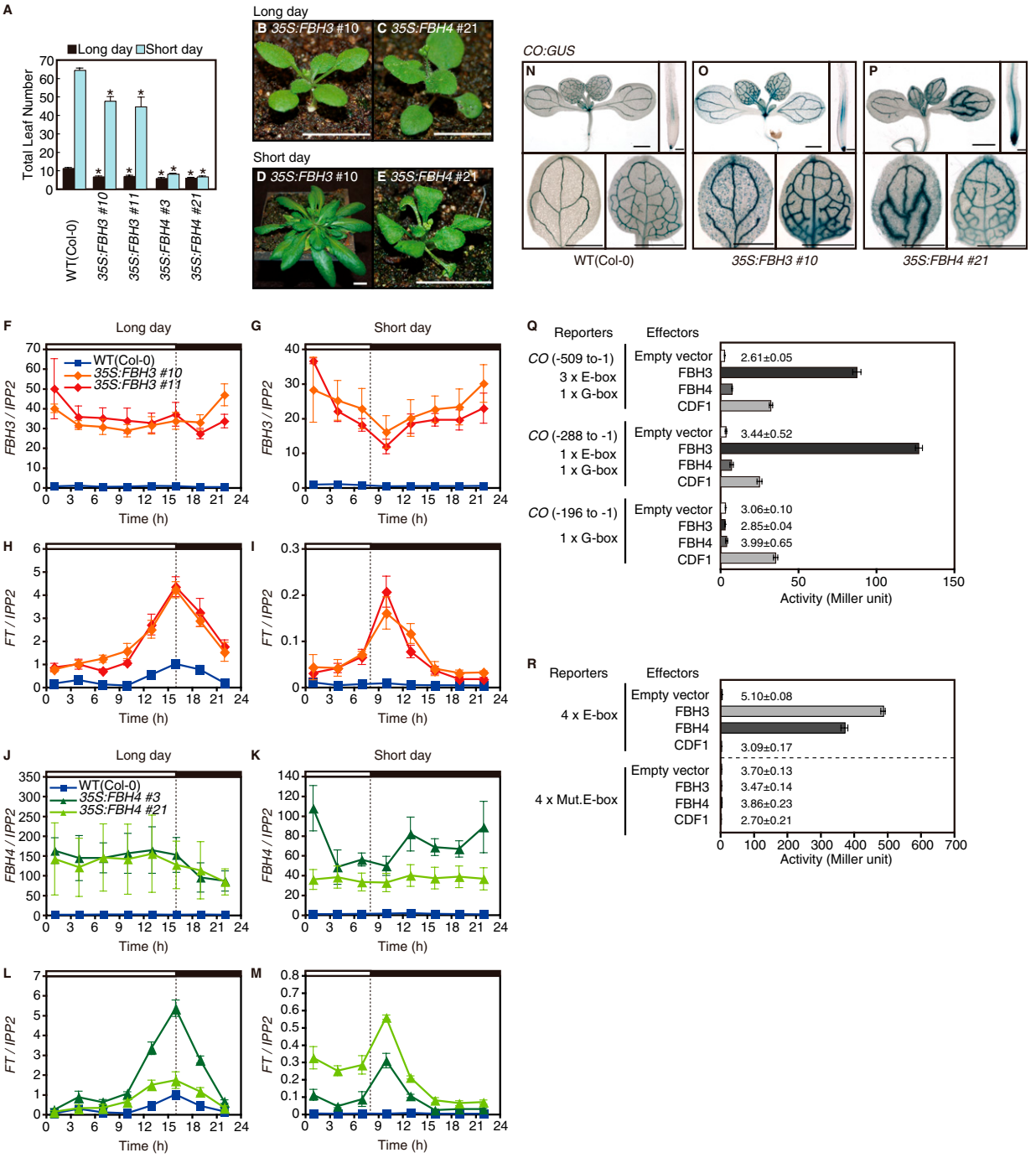

Fig. S4. FBH3 and FBH4 function as *CO* transcriptional activators. (*A*) Flowering phenotypes of plants overexpressing *FBH3* (*35S:FBH3*) and *FBH4* (*35S:FBH4*) under different photoperiods. *35S:FBH3* (#10 and #11) and *35S:FBH4* (#3 and #21) lines and wild-type plants were grown in both LD and SD, and then the total leaf number was counted. Error bars denote the SEM of at least eight plants per line. Asterisks (*) denote significant difference ($P < 0.001$) between each overexpressor and wild-type plants. The experiments were repeated at least twice, and similar results were obtained. Representative images of the *35S:FBH3* and the *35S:FBH4* plants in LD (*B* and *C*) and SD (*D* and *E*). The pictures were taken just after the plants bolted. The *35S:FBH3* was 16 d old, and the *35S:FBH4* was 16 d old in LD. The *35S:FBH3* was 56 d old, and the *35S:FBH4* was 29 d old in SD. (Scale bars, 10 mm.) (*F*–*M*) Daily expression patterns of *FBH3* (*F* and *G*), FBH4 (*J* and *K*) *FT* (*H*, *I*, *L*, and *M*) in *35S:FBH3* (#10 and #11), *35S:FBH4* (#3 and #21) and wild-type plants were measured in LD and SD conditions. *FBH3* and *FBH4* levels were normalized to the average value in the wild type (the average value from all of the wild-type time points was set to 1). The *FT* levels were normalized to the maximum value in wild type (the maximum value of wild type was set to 1). Bars above the graphs represent light conditions during harvesting samples: white bars represent light periods and black bars represent dark periods. (*N*–*P*) Spatial expression patterns of *CO* gene in wild type, *35S:FBH3*, and *35SFBH4* plants. Twelve-day-old wild-type (*N*), *35S:FBH3* (*O*), and *35S:FBH4* (*P*) plants carrying the *CO:GUS* reporter gene. Whole-mount staining of seedlings, cotyledons, and first leaves is shown. (Scale bars, 0.5 mm.) Staining of root tips are shown with scale bars (0.1 mm). (*Q* and *R*) FBH3 and FBH4 bind to the *CO* promoter in yeast. (*Q*) Interaction of FBH3 and FBH4 with the *CO* promoter in yeast. Bars represent the β-galactosidase enzyme activities (Miller units) controlled by a truncated *CO* promoter fragment. (*R*) Interaction between FBH3 and FBH4 with E-box. Experimental details are the same as those given in the Fig. 1 legend.

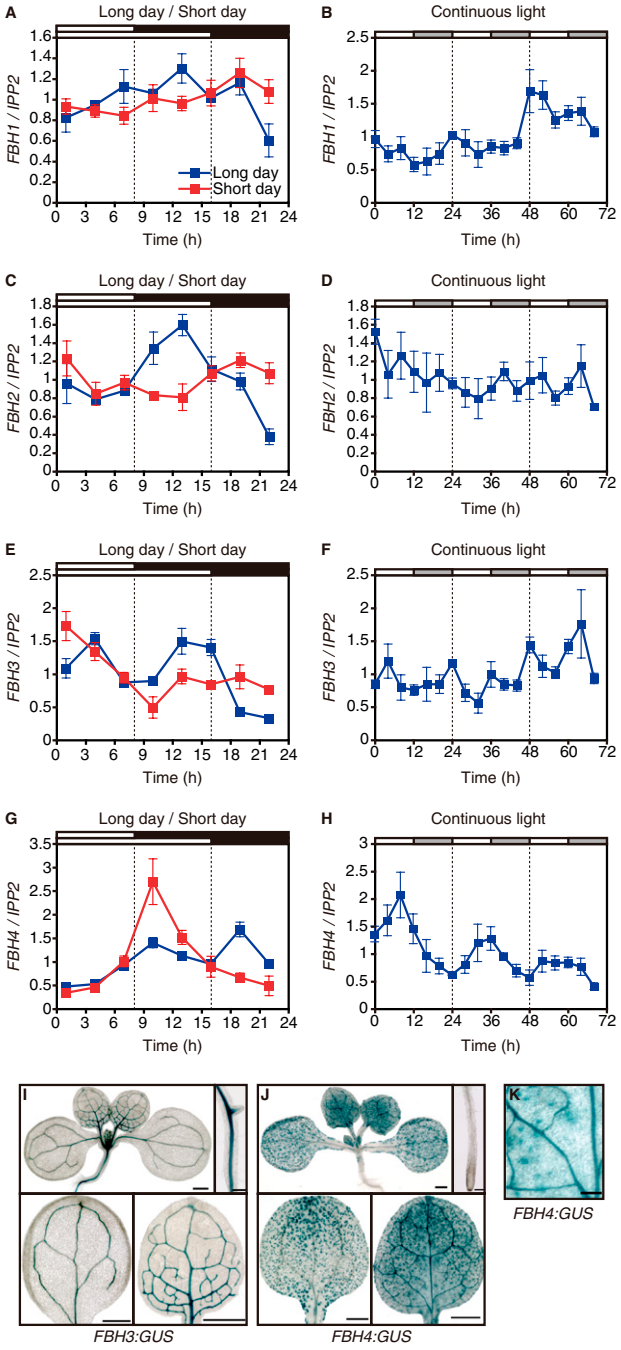

Fig. S5. Daily expression patterns of *FBH* in different photoperiod conditions and spatial expression patterns of *FBH*. (*A–H*) Daily expression patterns of *FBH1* (*A* and *B*), *FBH2* (*C* and *D*), *FBH3* (*E* and *F*), and *FBH4* (*G* and *H*) in wild-type plants were measured in LD, SD (*Left* panels in *A–H*), and continuous light (*Right* panels in *A–H*) conditions. Blue lines and red lines in the *Left* panels in *A–H* depict the results in LD and SD, respectively. Ten-day-old seedlings grown under 12-h light/12-h dark photoperiod conditions were transferred to continuous light conditions. The seedlings were harvested starting at the onset of light (ZT 0) and then at 4-h intervals for 3 d. All of the *FBH* levels were normalized to the average value in the wild type (the average value from all of the wild-type time points was set to 1). Bars above the graphs represent light conditions during harvesting samples: white bars represent light periods, black bars represent dark periods, and gray bars represent subjective night periods. (*I–K*) Spatial expression pattern of *FBH3* and *FBH4* was determined by histochemical staining for GUS activity using plants expressing *FBH3:GUS* (*I*) and *FBH3:GUS* (*J* and *K*) transgenic reporter genes. Whole-mount staining of seedlings, cotyledons, and first true leaves is shown. [Scale bars: 0.5 mm (*I* and *J*); 0.1 mm (*K*).]

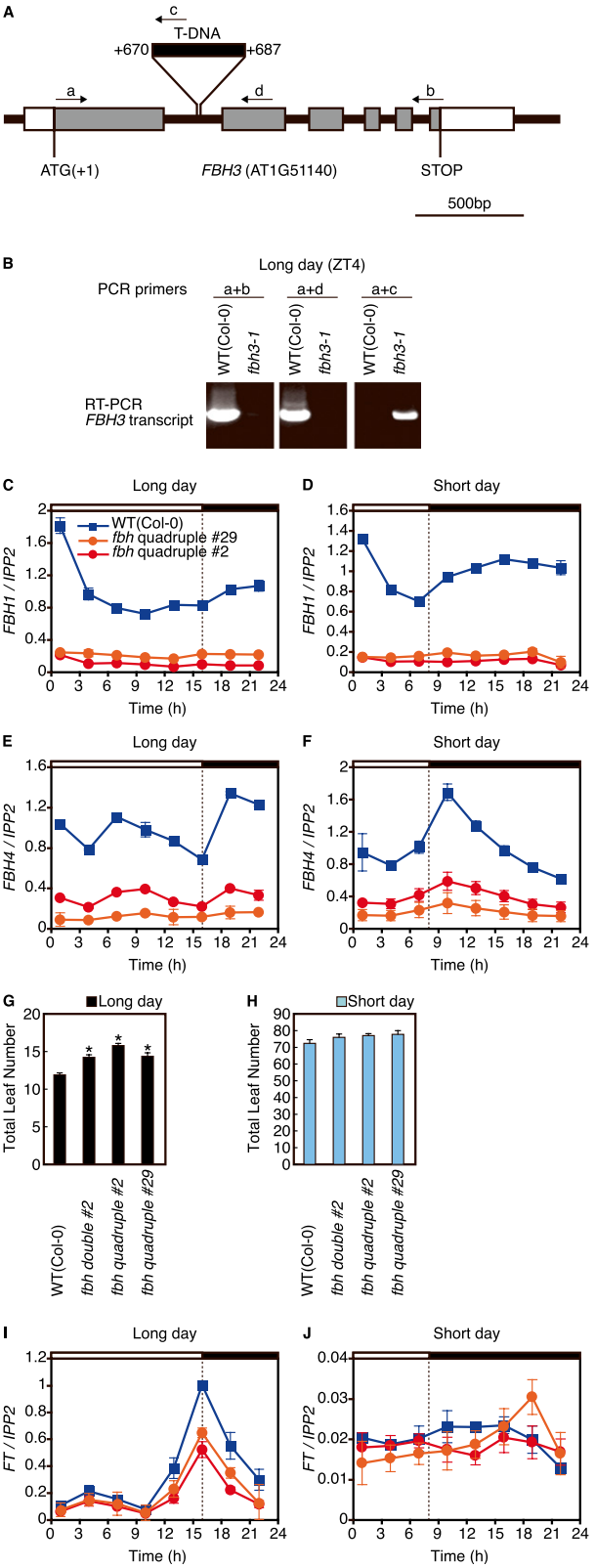

Fig. S6. The phenotype of two independent *fbh1 fbh2 fbh3 fbh4* quadruple mutants. (*A*) The *fbh3-1* T-DNA insertional mutant. Schematic representation of the *FBH3* locus in the *fbh3-1* mutant. A T-DNA is inserted at the first intron of *FBH3* gene, which is 670 bp downstream of the *FBH3* translation start site. The position and direction of primers that are used for RT-PCR analysis are shown. (*B*) RT-PCR analysis was performed on wild-type and *fbh3-1* seedlings harvested at ZT 4 in LD. We could not detect any intact *FBH3* transcripts in the *fbh3-1* mutant by RT-PCR analysis. Daily expression patterns of *FBH1* (*C* and *D*), *FBH4* (*E* and *F*), and *FT* (*I* and *J*) were measured in the *fbh* quadruple mutants (#29 and #2) and wild-type plants in LD and SD. *FBH1* and *FBH2* levels were normalized to the average value in the wild type (the average value from all of the wild-type time points was set to 1). The *FT* levels were normalized to the maximum value in

Legend continued on following page

wild type (the maximum value of wild-type in LD was set to 1). Bars above the graphs represent light conditions during harvesting samples: white bars represent light periods and black bars represent dark periods. Values represent means ± SEM from three biological replicates. (*G* and *H*) Flowering phenotype of *fbh* quadruple-mutant (#2 and #29), *fbh1 fbh2* double-mutant, and wild-type plants in different photoperiods. The seedlings were grown in LD and SD conditions, and the total leaf number was counted. Error bars denote the SEM of at least eight plants per each line. Asterisks (*) denote significant difference ($P < 0.001$) between each multiple *fbh* mutant plant and wild-type plants. The experiments were repeated at least twice, and similar results were obtained.

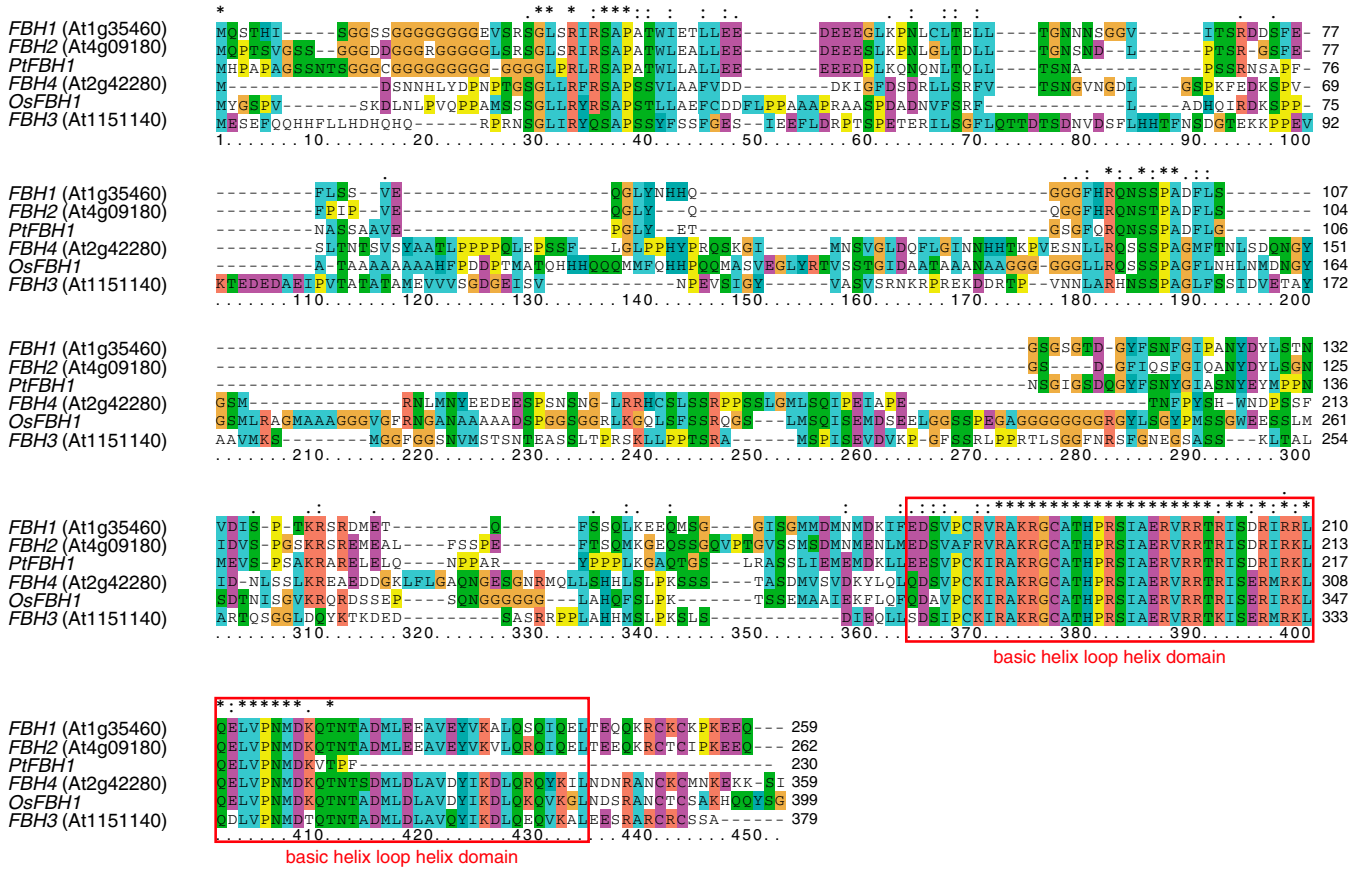

Fig. S7. FBH homologs in poplar and rice. Alignment of the full-length amino acid sequences of FBH1, FBH2, FBH3, FBH4, and FBH homologs in poplar and rice. *Pt*FBH1 (estExt_fgenesh4_pg.C_410126) is the closest FBH1 homolog in poplar on the basis of phylogenetic analysis (22). *Os*FBH1 (Os08g39630) is the rice FBH homolog, which is more similar to FBH3 and FBH4 on the basis of phylogenetic analysis (22). Conserved bHLH domains are outlined by red boxes. Identical amino acids are marked by asterisks (*) on top of the alignment. The alignment was generated by the MAFFT program (http://mafft.cbrc.jp/alignment/software/).

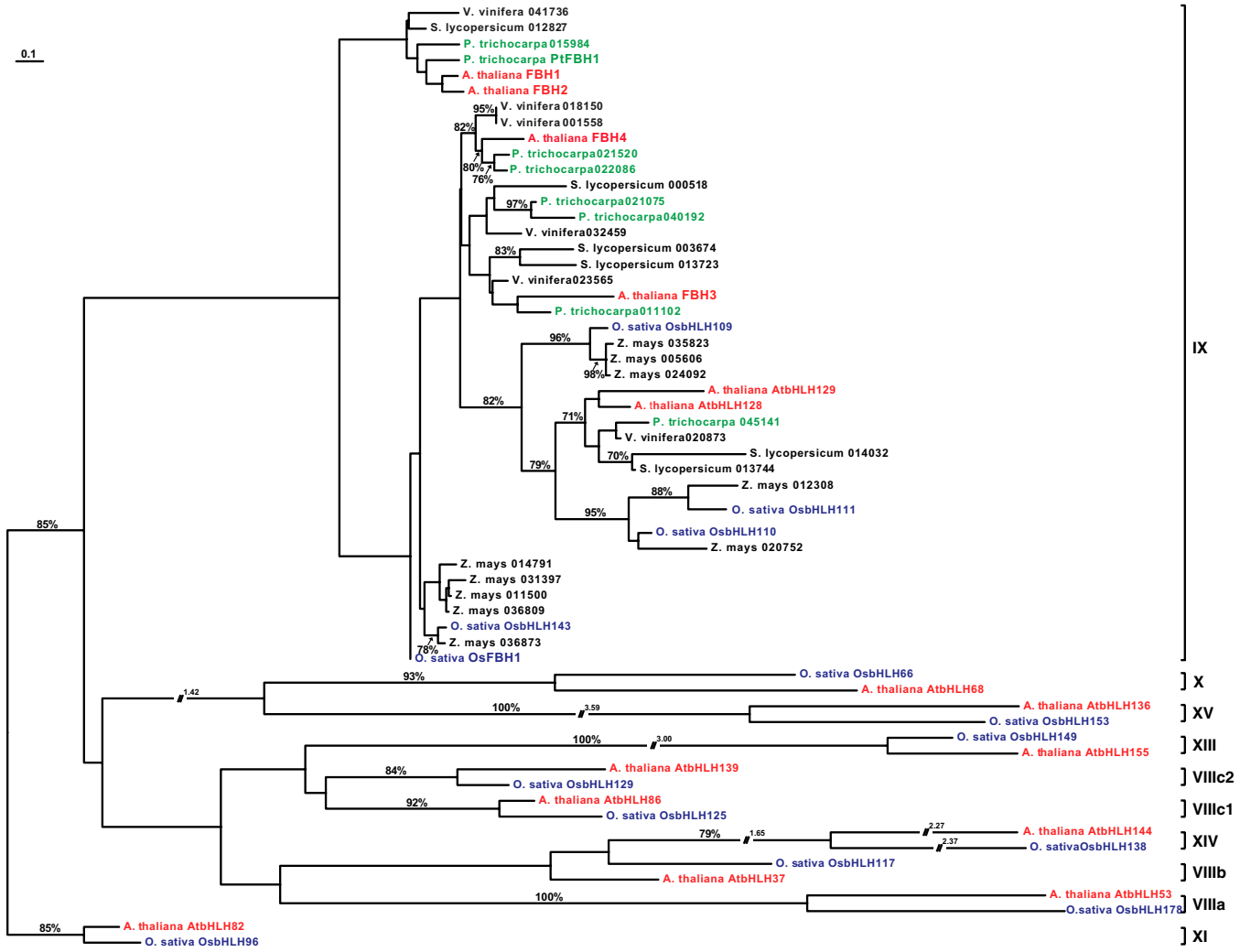

Fig. S8. Maximum-likelihood tree of bHLH proteins with bootstrap percentages of 100 pseudoreplicates are included above branches to show support values ≥70% for individual clades. Clades and *Arabidopsis* and rice bHLH nomenclatures are based on ref. 16. bHLH amino acid sequences derived from *Arabidopsis*, rice, and poplar genomes are shown in red, blue, and green, respectively. The bHLH amino acid sequences of each plant species are obtained from the following Web sites: *A. thaliana*, http://www.arabidopsis.org/; *O. sativa*, http://rice.plantbiology.msu.edu; *P. trichocarpa*, http://www.phytozome.net; *Solanum lycoperisicum*, http://www.plantgdb.org/; and *Zea mays* and *Vitis vinfera*, http://www.gramene.org and http://www.ncbi.nlm.nih.gov/. A six-digit number after each species name is an ID number of a transcription factor in the Plant Transcription Factor Database (http://planttfdb.cbi.pku.edu.cn/index.php). All FBH homologs are found in clade IX (16).

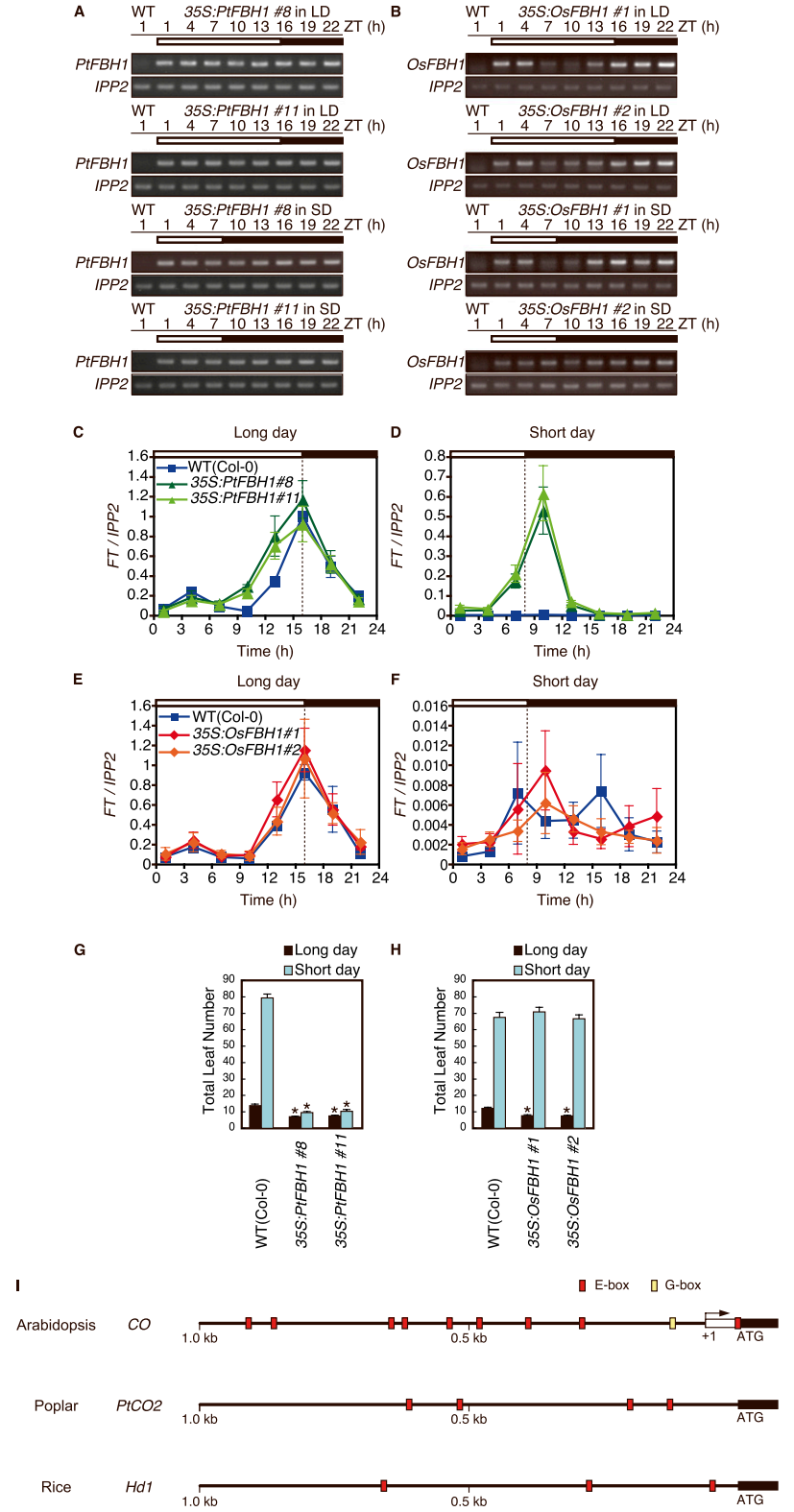

Fig. S9. The phenotype of *35S:PtFBH1* and *35S:OsFBH1* transgenic plants. (*A* and *B*) *PtFBH1* and *OsFBH1* transcripts were measured in transgenic *Arabidopsis* plants expressing *35S:PtFBH1* (#8 and #11) and *35S:OsFBH1* (#1 and #2) in LD and SD by RT-PCR. *IPP2* levels are shown as internal controls. (*C*–*F*) Daily expression patterns of *FT* in *35S:PtFBH1* (#8: and #11), *35S:OsFBH1* (#1: and #21), and wild-type plants were measured in LD and SD. *FT* levels were normalized to the highest value of the wild type in LD (the maximum value of wild type in LD was set to 1). Bars above the graphs represent light conditions during harvesting samples: white bars represent light periods and black bars represent dark periods. Values represent means ± SEM from three biological replicates. (*G* and *H*) Data on flowering phenotypes of plants overexpressing *PtFBH1* and *OsFBH1* under different photoperiods. *35S:PtFBH1* (#8 and #11), *35S:OsFBH1* (#1 and #2), and wild-type plants were grown in LD and SD, and the total leaf number was counted when they bolted. Error bars denote the SEM of at least eight plants per line. Asterisks (*) denote a significant difference ($P < 0.001$) between each overexpressor and wild-type plants. The experiments were repeated at least twice,

Legend continued on following page

and similar results were obtained. (*I*) E-box elements in the promoters of *CO* orthologs in poplar and rice. The positions of the E-box and G-box elements in 1 kb of the promoter regions of *CO* (*Arabidopsis*), *PtCO2* (poplar), and *Hd1* (rice) are indicated by red and yellow boxes, respectively. Within the regions, there are no G-box elements in the *PtCO2* and *Hd1* genes.

Table S1. Primers sequences used in this study: Artificial microRNA constructs

Construct	Primer name	Sequence[†] (5′–3′)
FBH1-1	miRFBH1-1 I miR-s	gaTAAATATCAACGTTGGTCGAGtctctcttttgtattcc
	miRFBH1-1 II miR-a	gaCTCGACCAACGTTGATATTTAtcaaagagaatcaatga
	miRFBH1-1 III miR*s	gaCCCGACCAACGTAGATATTTAtcacaggtcgtgatatg
	miRFBH1-1 IV miR*a	gaTAAATATCTACGTTGGTCGGGtctacatatatattcct
FBH1-2	miRFBH1-2 I miR-s	gaTAAATAGTCATAATTCGCCGCtctctcttttgtattcc
	miRFBH1-2 II miR-a	gaGCGGCGAATTATGACTATTTAtcaaagagaatcaatga
	miRFBH1-2 III miR*s	gaGCAGCGAATTATGTCTATTTTtcacaggtcgtgatatg
	miRFBH1-2 IV miR*a	gaAAAATAGACATAATTCGCTGCtctacatatatattcct
FBH4-2	miRFBH4-1 I miR-s	gaTTCGAATTTAGGTGAACGCAGtctctcttttgtattcc
	miRFBH4-1 II miR-a	gaCTGCGTTCACCTAAATTCGAAtcaaagagaatcaatga
	miRFBH4-1 III miR*s	gaCTACGTTCACCTATATTCGATtcacaggtcgtgatatg
	miRFBH4-1 IV miR*a	gaATCGAATATAGGTGAACGTAGtctacatatatattcct
FBH4-3	miRFBH4-3 I miR-s	gaTTTGGAATTAGATGGACTCTGtctctcttttgtattcc
	miRFBH4-3 II miR-a	gaCAGAGTCCATCTAATTCCAAAtcaaagagaatcaatga
	miRFBH4-3 III miR*s	gaCAAAGTCCATCTATTTCCAATtcacaggtcgtgatatg
	miRFBH4-3 IV miR*a	gaATTGGAAATAGATGGACTTTGtctacatatatattcct

[†]The regions encoding microRNAs specific to each target mRNA are shown in capital letters.

Table S2. Primers sequences used in this study: Quantitative PCR primer sequences

Gene	Primer name	Sequence (5′–3′)
GI	qGI-F	GGGTAAATATGCTGCTGGAGA
	qGI-R	CAGTATGACACCAGCTCCATT
IPP2	qIPP2-F	GTATGAGTTGCTTCTCCAGCAAAG
	qIPP2-R	GAGGATGGCTGCAACAAGTGT
CO	qCO-F	CTACAACGACAATGGTTCCATTAAC
	qCO-R	CAGGGTCAGGTTGTTGC
FT	qFT-F	CTGGAACAACCTTTGGCAAT
	qFT-R	TAC ACT GTT TGC CTG CCA AG
CDF1	qCDF1-F	TTTCCCGACGGTTTTAGAGG
	qCDF1-R	CCATGCTGTTGCATCTTGGA
CDF2	qCDF2-F	GAACCCAATGAAGGCTTGAA
	qCDF2-R	GGAACCAGATGGTGAATTGG
FBH1	qFBH1-2F	ATCAAGGTGGTGGCTTTCAC
	qFBH1-2R	TAATTCGCCGGAATACCAAA
FBH2	qFBH2-1F	TTGGGATTCAGGCGAATTAC
	qFBH2-1R	TAGGAACTTGACCGCTGCTT
FBH3	qFBH3-F	TGCCTCCTCGGACGCTTTCCGGTGG
	qFBH3-R	CTACTTGCTGAATCCTCATCCTTGG
FBH4	qFBH4-F	ATCCTCACTTAAAAGAGAAGCCGAG
	qFBH4-R	TGTAGCTGAAGATACTTATCCACTG
FLC	qFLC-F2	CCGAACTCATGTTGAAGCTTGTTGAG
	qFLC-R2	CGGAGATTTGTCCAGCAGGTG
SOC1	qSOC1-F2	AGCTGCAGAAAACGAGAAGCTCTCTG
	qSOC1-R2	GGGCTACTCTCTTCATCACCTCTTCC

Table S3. Primers sequences used in this study: CO amplicons for ChIP assay

Amplicon (position*)	*cis*-elements†	Primer name	Sequence (5′–3′)
1 (−2045 to −1846)	3 E-box	*CO* amplicon 27F	CGTTAATCTGAAAGAAGCAAAGTATTC
		CO amplicon 27R	TAATTAAGTTTATTGTTGTAGCGG
2 (−1846 to −1677)	1 E-box	*CO* amplicon 28F	GAGACTGTCAACGAGCAATAATAAGC
		CO amplicon 28R	TGCCAAGTTGGATAAGTTGAGGC
3 (−1495 to −1290)	1 E-box	*CO* amplicon 6F	AAGTTCAAAATGGGAAAGAGAAGTG
		CO amplicon 6R	TGATACCCATTATGTGGTCCAAAA
4 (−858 to −654)	2 E-box	*CO* amplicon 8F	TGGTTACCAAGTGCAAATTTCTACA
		CO amplicon 8R	GAGAATCATATCGGAAAAGTGACATGAA
5 (−430 to −273)	1 E-box	*CO* amplicon 21F	GAACAGTAATCACAAGGTTCAGG
		CO amplicon 21R	ATGGTGTTGCAGGCAAATTGTTAC
6 (−301 to −89)	1 E-box	*CO* amplicon 10F	AATAGTAACAATTTGCCTGCAACAC
		CO amplicon 10R	TTATTGGATCCTCTTGCAGCTAGT
7 (−89 to +66)	1 E-box 1 G-box	*CO* amplicon 23F	CATGTAAGAGCCACTAACGC
		CO amplicon 23R	AACATAATAACTCAGATGTAGTAAG
8 (+492 to +709)	1 E-box	*CO* amplicon 13F	TGATAAGGATGCCAAGGAGGTT
		CO amplicon 13R	AAGCGGAACAACTCTATCTCCC
9 (+2784 to +2947)	—	*CO* amplicon 25F	GACGGCCCAAGTAGTCTTCCG
		CO amplicon 25R	GTGCAATTATGAAGTTCGTTGTCG

*The *CO* transcriptional start site was counted as +1.
†The number of the E-box or the G-box in the genomic region corresponding to each amplicon is indicated.